

## Effect of the Solids Inventory and Fluidization Gas Velocity on the Hydrodynamics of a Circulating Fluidized Bed

Flavia Tramontin Silveira Schaffka<sup>a,\*</sup>, Jhon Jairo Ramirez Behainne<sup>b</sup>, Maria Regina Parise<sup>c</sup>, Guilherme José de Castilho<sup>a</sup>

<sup>a</sup>School of Chemical Engineering, University of Campinas (UNICAMP), Campinas, Brazil

<sup>b</sup>Mechanical Engineering Department, Federal University of Technology (UTFPR), Ponta Grossa, Brazil

<sup>c</sup>Chemical Engineering Department, Federal University of Technology (UTFPR), Ponta Grossa, Brazil

[flatramontim@hotmail.com](mailto:flatramontim@hotmail.com)

The hydrodynamics behavior of a bench-scale circulating fluidized bed (CFB) system has been analyzed in terms of the axial pressure profile and solids circulation rate. Experimental runs were carried out at room conditions using beds of quartz sand and air as the fluid phase in order to know the effect of the overall solids inventory and the superficial gas velocity used in the riser. Static pressure signals obtained from the gas-particle flow were registered at several positions along the CFB loop and the solids circulation rate was measured by using a diverter valve installed at the standpipe section. A statistical analysis applied on the experimental data show that the solids inventory and the superficial gas velocity in the range here studied lead to significant changes on the hydrodynamics of the circulating fluidized bed system.

Keywords: Circulating fluidized bed riser, gas-particle hydrodynamics, static pressure signals, solids circulation rate.

### 1. Introduction

Circulating fluidized bed reactors (CFB) have been widely used in industrial processes due to the intense multiphase interaction that they promote under the fast fluidization regime. Inside of a CFB riser the fast fluidization regime leads to non-uniform solid concentration along the column in the presence of a high mixture of solids and significant slip gas-particle velocities. Therefore, a relatively dense bed at the riser bottom as well as a more dilute zone with clusters near the wall at upper regions of the riser become evident (Bai et al., 1996; Basu, 2006). Previous works have pointed out that the gas-solid hydrodynamics in CFB systems is driven by the static pressure balance around the CFB loop, which can be mainly influenced by the particle properties, the superficial gas velocity, the overall solids inventory, the operation of the solids circulation valve and the geometrical features of the CFB system.

In this way, Basu and Cheng (2000) showed details about the pressure balance behavior as influenced by the loop-seal operation. Kim et al. (2002) proposed a pressure balance model in a CFB system provided with loop-seal and an abrupt riser outlet that agreed well with their experimental data. Kim et al. (2004) studied the axial pressure profile under transition condition from fast fluidization regime to pneumatic transport in a riser. Grieco and Marmo (2008) analyzed the pressure drop across the riser at low solid circulation rates. Qi et al. (2008) looked into the effects of particle diameter, particle density and gas distributor design on the CFB hydrodynamics. Yao et al. (2011) verified that the gas-solid flow in the standpipe region significantly impacts the pressure balance. Lim et al. (2012) showed how the CFB hydrodynamics can be affected when the solids circulation rate changes in function of both the superficial gas velocity in the riser and the overall solids inventory. Wang and Fan (2015) also found that the solids circulation rate impacts on the pressure distribution. Karlsson et al. (2017) studied the solids circulation rate behavior in CFBs with low riser aspect ratio and varying the total solids inventory. It was found that the solids circulation rate is determined by the solids concentration at the top of the riser, which in turn depends on the pressure drop and the fluidization gas velocity in the vessel, as well as by the loop-seal operating conditions and the backflow effect that the

geometry of the riser exit region promotes. Recently, Zhou et al. (2018) analyzed the pressure balance and the solids circulation rate behavior in dual circulating fluidized bed (DCFB) reactors. This study investigated the effects of specific operating parameters on pressure balance and solid circulation rate, including the overall solids inventory, the riser gas velocity, the bubbling fluidized bed gas velocity and the seal pot gas velocity. It was found that relevant operating parameters can be adjusted to control the pressure distribution and the solid circulation rate in different parts of the system, in order to ensure the safe and stable operation of DCFB reactors.

The aforementioned works suggest that the hydrodynamics of the CFB systems need further studies due to their distinctive scale up and geometry, particle properties and specific operating features. Unlike previous studies, the present work brings the application of the statistical analysis to assess the influence of the total solids inventory and the fluidization gas velocity on the axial pressure profile and the solids circulation rate in different operation conditions of a bench-scale CFB system.

## 2. Material and Methods

Particles of quartz sand (Geldart Group B) were used as the bed material. The particle properties are showed in Table 1.

Table 1. Properties of the bed particles

Particle	Sauter diameter, $d_p$ ( $\mu\text{m}$ )	Size range ( $\mu\text{m}$ )	Density, $\rho_p$ ( $\text{kg}/\text{m}^3$ )	Sphericity, $\Phi$ (-)	Minimum superficial air velocity (m/s) *	Transport velocity (m/s) **	Geldart group
Quartz sand	$272 \pm 7$	210-300	2657.1	$0.729 \pm 0.148$	0.125	3.26	B

\*Obtained from Ergun equation (Basu, 2006); \*\* Calculated by equation from Basu (2006).

The Sauter mean diameter of the particles was obtained by using a laser diffraction particle size analyzer (Mastersizer S, Malvern model S-MAM 5005). The absolute density was determined by using an automatic gas pycnometer (AccuPyc 1330, manufactured by Micromeritics Instrument Corporation). The determination of the particle sphericity followed the Peçanha and Massarani (1986) method, which consists of the ratio between the inscribed and circumscribed particle diameter from photographs caught with Scanning Electron Microscopy (LEO Electron Microscopy/Oxford, model MEV Leo 440i, Leo software v03.01).

The experimental runs were performed in a bench-scale CFB system made of carbon steel and Plexiglass. The apparatus is composed of a riser with 0.078 m inner diameter and 2.7 m height, a high efficiency tangential cyclone, a standpipe, and an U-type loop-seal used as the solid recycle device (Fig. 1). The fluidization air fed into the riser is moved by a radial blower coupled to an electric motor (4.0 hp), which is driven by a frequency inverter to control the shaft rotation velocity. A RTD (PT-100) sensor is used to measure the temperature of the fluidization air. The air flow rate supplied to the bed is determined by an orifice plate meter built from ISO Standard NBR 5167-1 (ABNT, 1998), with 0.030 m of hole diameter. The pressure drop across the orifice plate and the up-wind pressure of the gas were measured by two differentials pressure transducers (range from 0 to 6,221 Pa and from 0 to 24,884 Pa, respectively). An air distributor with seven perforated tuyères is placed at the bottom of the riser.

Differential pressure transducers in the range from 0 to 12,442 Pa were distributed around the CFB loop (riser, cyclone, standpipe and loop seal valve). A diverter valve is installed in the standpipe section to measure the solids circulation rate. An U-type loop-seal valve made of Plexiglass is connected at the bottom zone of the standpipe section. The supply chamber and the recycle chamber of the loop-seal valve have square cross section (width of 0.059 m). The aeration in the loop-seal valve is supplied by a screw-type compressor (25 hp). Two rotameters assembled in parallel (range from 2 to 22 sL/min) were used to measure the aeration flow rate fed into the loop-seal valve.

The signals obtained from the pressures transducers were recorded by a data acquisition system and processed by using the LabVIEW<sup>TM</sup> software. Each run of the experimental plan was replicated in order to improve the significance of the experimental results.

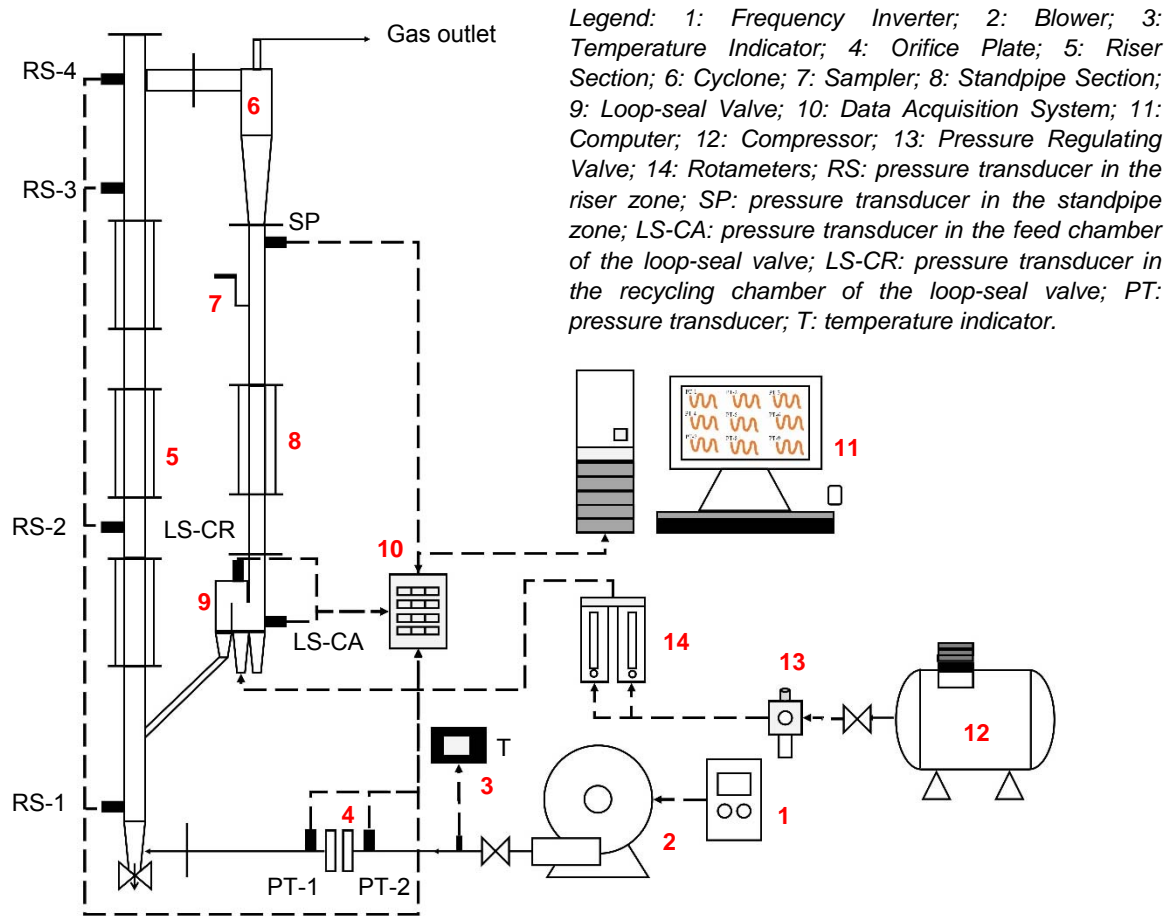


Figure 1: Experimental system.

The axial pressure profiles were obtained from the local mean static pressure values measured in the respective CFB section. In addition, for each experimental test, four samples were collected to determine the mean solids circulation rate ( $G_s$ ), which was calculated by Eq. (1):

$$G_s = \frac{m_s}{A_r \cdot t} \quad (1)$$

where  $m_s$  is the mass of solids caught in the diverter valve;  $A_r$  is the cross-section area of the riser, and  $t$  is the sampling time (6 s).

The experimental runs followed a  $3^2$  factorial design. The controlled factors were the overall solids inventory and the superficial air velocity, as resumed in Table 2.

Table 2. Controlled factors used in experiments.

Factor			
Overall solids inventory		Superficial air velocity	
Value (kg)	Level	Value (m/s)	Level
4.0	(-1)	3.4	(-1)
4.5	(0)	3.8	(0)
5.0	(+1)	4.2	(+1)

The response variables were the static pressure drop and the solids circulation rate. The aeration flow rate in the loop-seal valve was kept constant at 24 sL/min in all experimental runs.

### 3. Results and Discussion

Figure 2 (a, b and c) shows the axial pressure profile assessing the effect of the superficial air velocity ( $u_0$ ) under different overall solids inventory ( $I_s$ ) values. In these conditions, the static pressure values increase when the superficial air velocity also goes up because increasing  $u_0$  generates greater friction forces of the gas-solid suspension with the pipe walls. Some studies report that, for small-scale circulating fluidized beds, the pressure level in the riser depends not only on the weight of the particles but also on the friction between the gas and the particles as well as the friction between the particles and the riser walls. So, under the other operating conditions of this work, the axial profiles are consistent with those observed in previous studies (Kim et al., 2002; Goo et al., 2008; Wang e Fan, 2015; Rahman et al., 2017; Zhou et al., 2018).

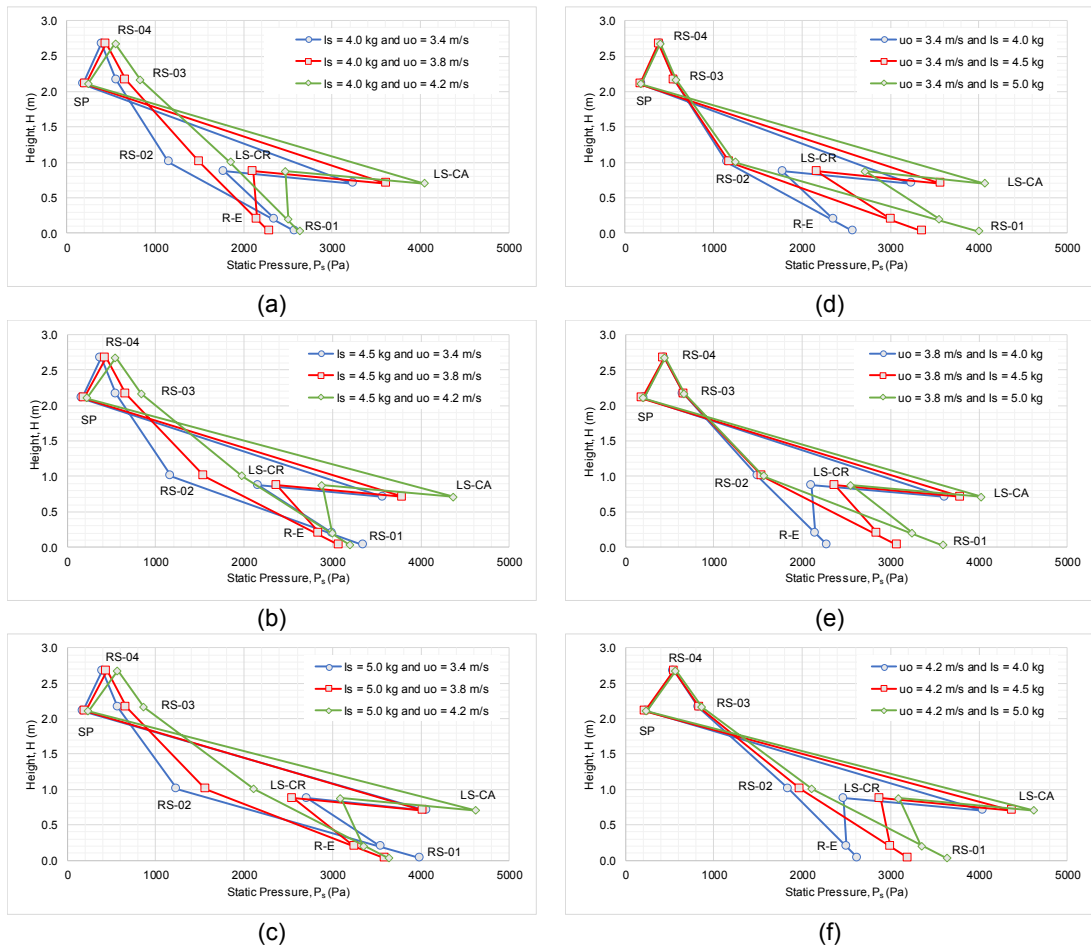


Figure 2: Axial pressure profile. Operation conditions: Effect of the superficial air velocity: (a)  $I_s = 4.0$  kg, (b)  $I_s = 4.5$  kg, (c)  $I_s = 5.0$  kg; Effect of the overall solids inventory: (d)  $u_0 = 3.4$  m/s, (e)  $u_0 = 3.8$  m/s, (f)  $u_0 = 4.2$  m/s.

Figure 2 (d, e and f) shows the axial pressure profile in terms of the variations of the overall solids inventory under different  $u_0$  values. The increase of the overall solids inventory in the system, keeping the other operation conditions constant, leads to higher static pressure values in each component of the CFB loop, once that this increase of the inventory imposes a new condition of equilibrium to the system, as observed in other works (Kim et al., 2002; Goo et al., 2008; Wang e Fan, 2015; Rahman et al., 2017; Zhou et al., 2018). The reason for this occurrence is explained by the increase in the solids holdup of the bed with more mass of solids in the system. In this way, the pressure balance is maintained, correcting itself automatically for higher values of solids inventory.

The thickness of the clusters (particle agglomeration) in the annular zone varies along the riser and it depends on the superficial air velocity and the solids circulation rate. Due to the height of solids accumulated in the standpipe, the static pressure of the system also grows in the supply chamber side of the loop-seal valve. At the bottom zone (dense region) of the riser the differential pressure is higher than at the top of the column

(dilute region) as a result of the difference in the particle load supported in each region. In this way, the overall solids inventory put into the system affects the particles distribution in all components of the CFB loop.

Fig. 3 (a) shows that the solids circulation rate increases as the solids inventory also increases. Similarly, the increase in the solids circulation rate occurs with higher superficial air velocities (Fig. 3b). The solids circulation rate can be controlled by adjusting the riser gas velocity and the overall solids inventory, as demonstrated by Kim et al. (2002), Goo et al. (2008), Lim et al. (2012), Karlsson et al. (2017) and Zhou et al. (2018).

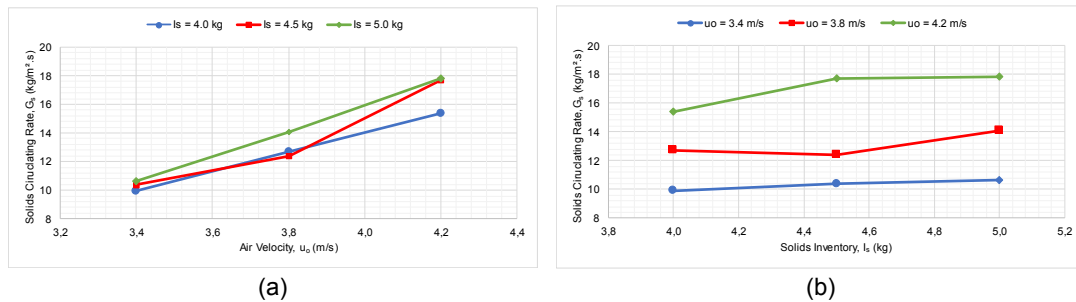


Figure 3: Solids circulation rate. Operation conditions: (a) Effect of the overall solids inventory; (b) Effect of the superficial air velocity.

A statistical analysis was also carried out to verify the significance (confidence level of the 95%) of the effect promoted by both factors (overall solids inventory and superficial air velocity) on the pressure drop in the riser and the solids circulation rate. By assessing the pressure drop in the riser, the Pareto chart (Fig. 4a) shows that solids inventory had significant effect and it is directly proportional to the pressure drop in the riser. On the other hand, the superficial air velocity was almost significant in the tested experimental range, indicating a negative value of the effect. It means that the higher the superficial air velocity, the lower the pressure drop in the riser. This result was expected, once the slip gas-particle velocity becomes smaller when the superficial air velocity increases beyond the transport velocity of solids, reducing the solids holdup and the particles agglomeration at the riser bottom. The pressure drop may become important under some operational and system scale situations, mainly involving relatively low suspension densities and reduced diameter of the fluidization columns (Basu, 2006). As for solids circulating rate, the Pareto chart (Fig. 4b) shows that the superficial air velocity is more significant compared to the solid inventory. In addition, the solids circulation rate increases with the increase of both factors.

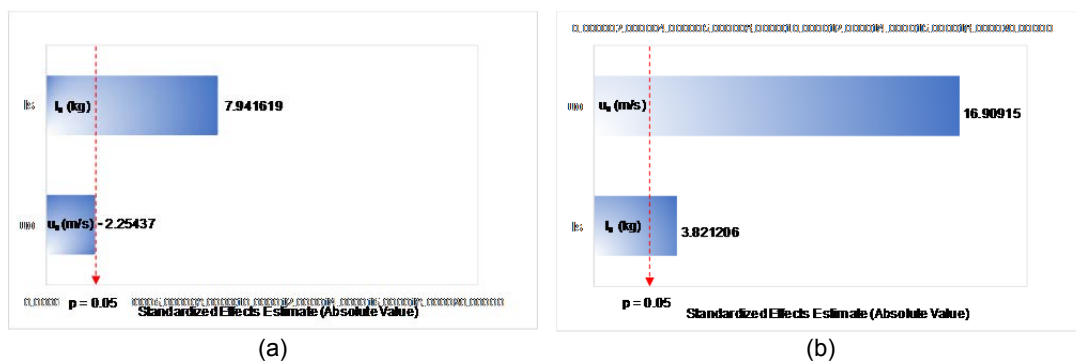


Figure 4: Pareto chart of standardized effects.  $3^2$  full factorial design with replicate (total of 18 runs); MS Pure Error = 0.4633056; Confidence level: 95%. (a) Pressure drop in the riser (Pa); (b) Solids circulation rate (kg/m<sup>2</sup>.s).

#### 4. Conclusions

Results of the axial pressure profiles in the circulating fluidized bed show that the ranges of the overall solids inventory and the superficial air velocity here studied lead to significant changes on the local static pressure. In these conditions, it was verified that the static pressure values in all components of the CFB loop increase

when the superficial air velocity and the solids inventory also increase. In addition, the statistical analysis revealed that the increase of both the superficial air velocity and the solids inventory leads to higher values of the solids circulation rate. For this operating parameter, the superficial air velocity presented greater significance effect than the solids inventory in the CFB system. On the other hand, it was found that the pressure drop in the riser goes down when the superficial air velocity increases or the mass of solids charged into the fluidization loop decreases. In this sense, the effect of the overall solids inventory was the most significance.

### Acknowledgments

This study was financed in part by the Coordenação de Aperfeiçoamento de Pessoal de Nível Superior - Brasil (CAPES).

### References

- Bai D., Shibuya E., Masuda Y., Nakagawa N., Kato K, 1996, Flow structure in fast fluidized beds, *Chemical Engineering Science*, 51, 957-966.
- Basu P., 2006, *Combustion and Gasification in Fluidized Beds*. Taylor & Francis Group.
- Basu P., Cheng L., 2000, An analysis of loop-seal operations in a circulating fluidized bed, *Chemical Engineering Research and Design*, 78, 991-998.
- Goo J.H., Seo M.W., Park D.K., Kim S.D., Lee S.H., Lee J.G., Song B.H., 2008, Hydrodynamic properties in a cold-model dual fluidized-bed gasifier, *Journal of Chemical Engineering of Japan*, 41, 7, 686-690.
- Grieco E., Marmo L., 2008, A model for the pressure balance of a low density circulating fluidized bed, *Chemical Engineering Journal*, 140, 414-423.
- Issangya A.S., Grace J. R., Bai D., Zhu J., 2000, Further measurements of flow dynamics in a high-density circulating fluidized bed riser, *Powder Technology*, 111, 104-113.
- Karlsson T., Liu X., Pallarès D., Johnsson F., 2017, Solids circulation in circulating fluidized beds with low riser aspect ratio and varying total solids inventory, *Powder Technology, China*, 316, 670-676.
- Kim S.W., Kim S.D., Lee D.H, 2002, Pressure Balance Model for Circulating Fluidized Beds with a Loop-seal. *Industrial & Engineering Chemistry Research, Korea*, 41, 20, 4949-4956.
- Kim S.W., Kirbas G., Bi H., Jim Lim C., Grace J.R., 2004, Flow behavior and regime transition in a high-density circulating fluidized bed riser, *Chemical Engineering Science*, 59, 3955-3963.
- Lim M.T., Pang S., Nijdam J., 2012, Investigation of solids circulation in a cold model of a circulating fluidized bed, *Powder Technology*, 226, 57-67.
- Qi X. B., Huang W.X., Zhu J., 2008, Comparative study of flow structure in circulating fluidized bed risers with FCC and sand particles, *Chemical Engineering Technology*, 31, 542-553.
- Peçanha R.P., Massarani G., 1986, Feature size and shape of particles. In: *Proceedings of the Fourth Meeting on the Flow in Porous Media, Campinas*, 14, 1, 302-312.
- Wang D., Fan L-S., 2015, L-valve behavior in circulating fluidized beds at high temperatures for group D particles, *Industrial & Engineering Chemistry Research*, 54, 4468-4473.
- Yao X., Zhang H.Y.H., Zhou C., Liu Q., Yue G., 2011, Gas-solid flow behavior in the standpipe of a circulating fluidized bed with a loop-seal, *Energy Fuels*, 25, 246-250.
- Zhou Y., Yang L., Lu Y., Hu X., Luo X., Chen H., Wang J., Yang Y., 2018, Control of pressure balance and solids circulation characteristics in DCFB reactors. *Powder Technology, China*, 328, 114-121.